Simplified shadow model of solar radiation pressure for GNSS satellites with large communication antenna

Kyohei Akiyama, Kaori Kawate, Yuki Igarashi, Toshitaka Sasaki, and Satoshi Kogure

Satellite Navigation Unit, JAXA

1st July 2024

SRP modeling for GNSS satellites

- Modeling of shadowing effect for Box-wing model
  - Analytical model to describe non-gravitational forces using only disclosed data
  - Necessary to correctly model the shadow cast by reflectors mounted on satellites in geostationary orbit (e.g., QZS-3 and BDS GEO)

- Concept
  - ✓ Easy to install to conventional box-wing model
  - ✓ Using only disclosed data

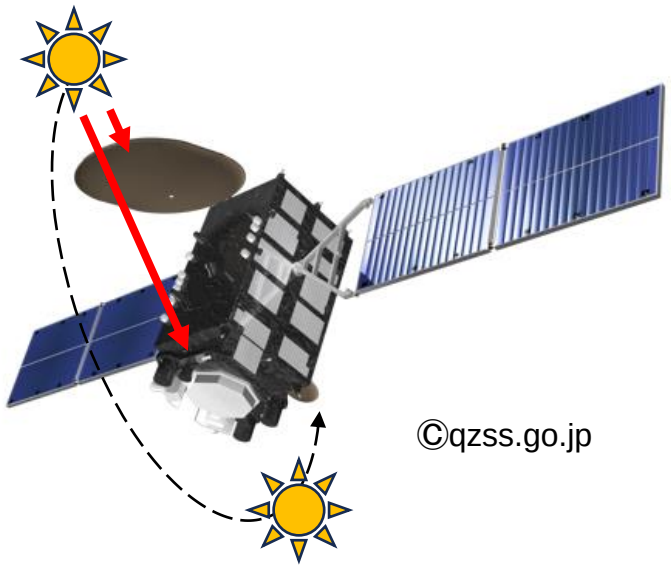

©qzss.go.jp

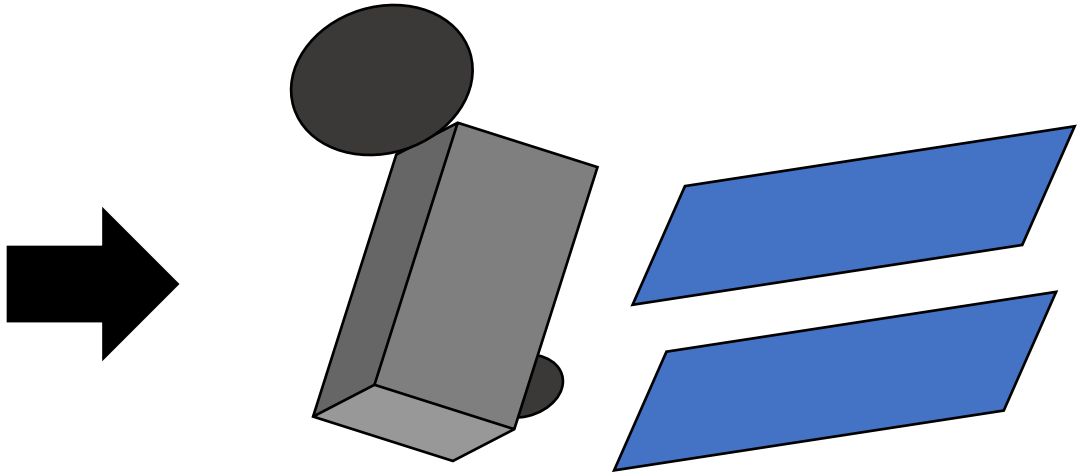

Simplified shadow model for QZS-3

- Algorithms
  - The effective area $\bar{A}_k$ of the surface k affected by the shadow considering the transmittance of the shielding structure τ_i (e.g., Reflector-1) is expressed by the following equation.

$$\bar{A}_k = A_k - (1 - \tau_i) \cdot f_k(\mu, \beta)$$

  - A_k is the surface area without shadow effect obtained using publicly available metadata.
  - $f_k(\mu, \beta)$ is a simplified shadow model for QZS-3's reflector-1, 2 and the +/-x body surface.

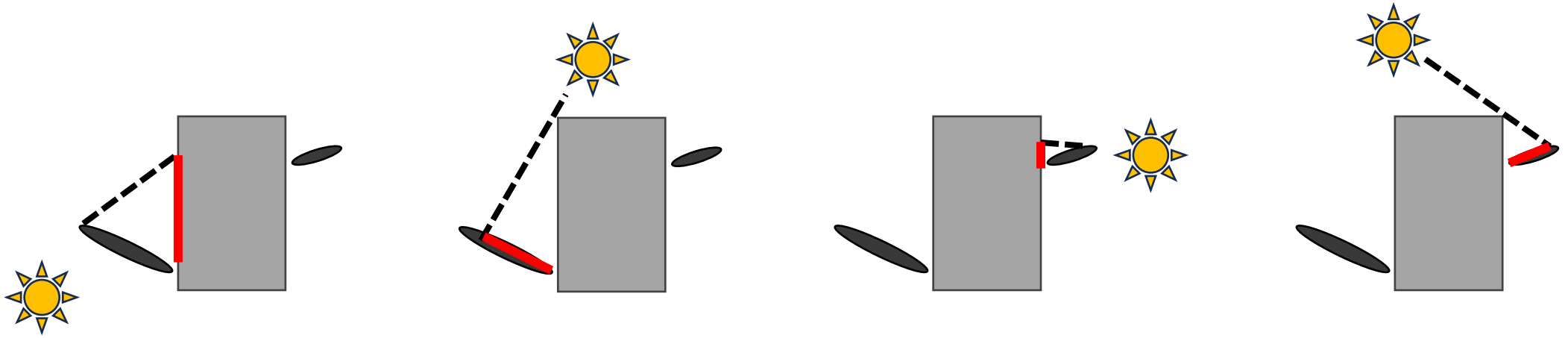

$f_{+\mathrm{xbody}}(\mu, \beta)$ $f_{\mathrm{ref1}}(\mu, \beta)$ $f_{-\mathrm{xbody}}(\mu, \beta)$ $f_{\mathrm{ref2}}(\mu, \beta)$

Simplified shadow model for QZS-3

- Sun direction relative to the body-fixed (BF) frame
  - For GNSS satellites in orbit normal (ON) mode, the azimuth angle and elevation angle relative to the X-Z plane of satellite BF frame can be expressed in terms of geocentric orbit angle μ and beta angle β
  - The rotation direction of the angle μ is counter-clockwise from the view of +y direction in satellite BF frame

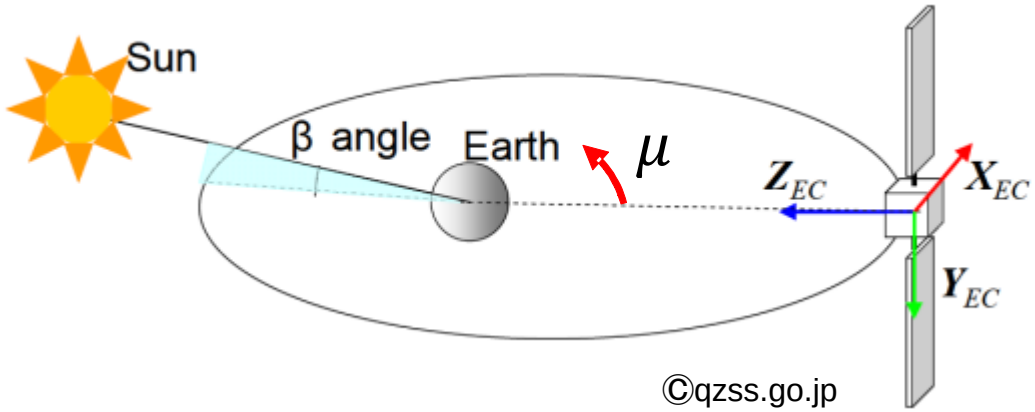

Orbit normal mode in ECI frame

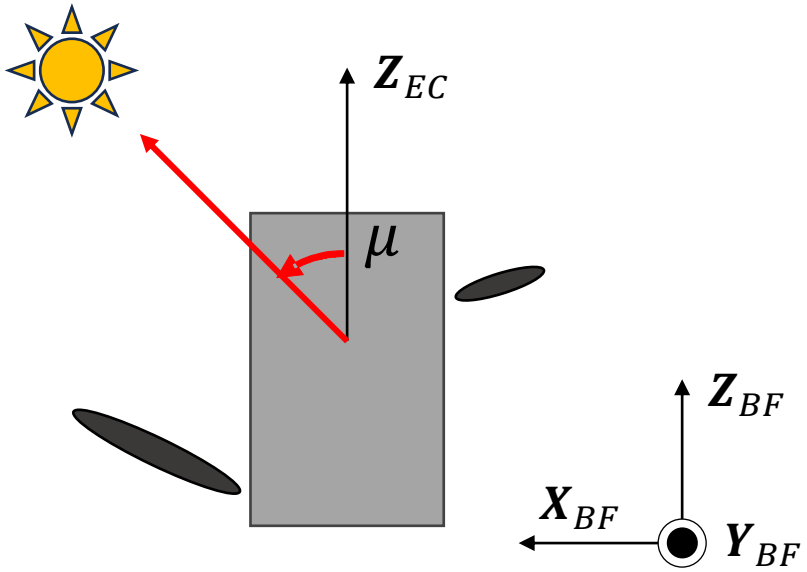

Body-fixed frame

Simplified shadow model for QZS-3

- Shape and orientation of the large antenna
  - The tilt angles of the reflector-1 and -2 with respect to the y-z plane of the body-fixed frame are considered (same direction as the angle μ).
  - The shape of the QZS-3's reflector-1 and -2 is assumed to be square whose area is equal to that of the circular reflector for simplification.
  - The gap between only the reflector-1 and the satellite body should be considered because sunlight shines through the gap.

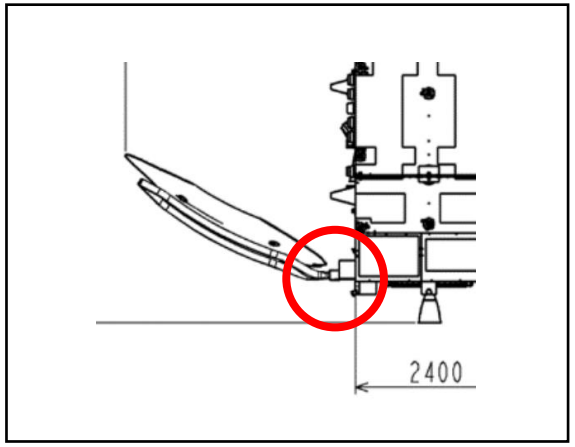

© qzss.go.jp

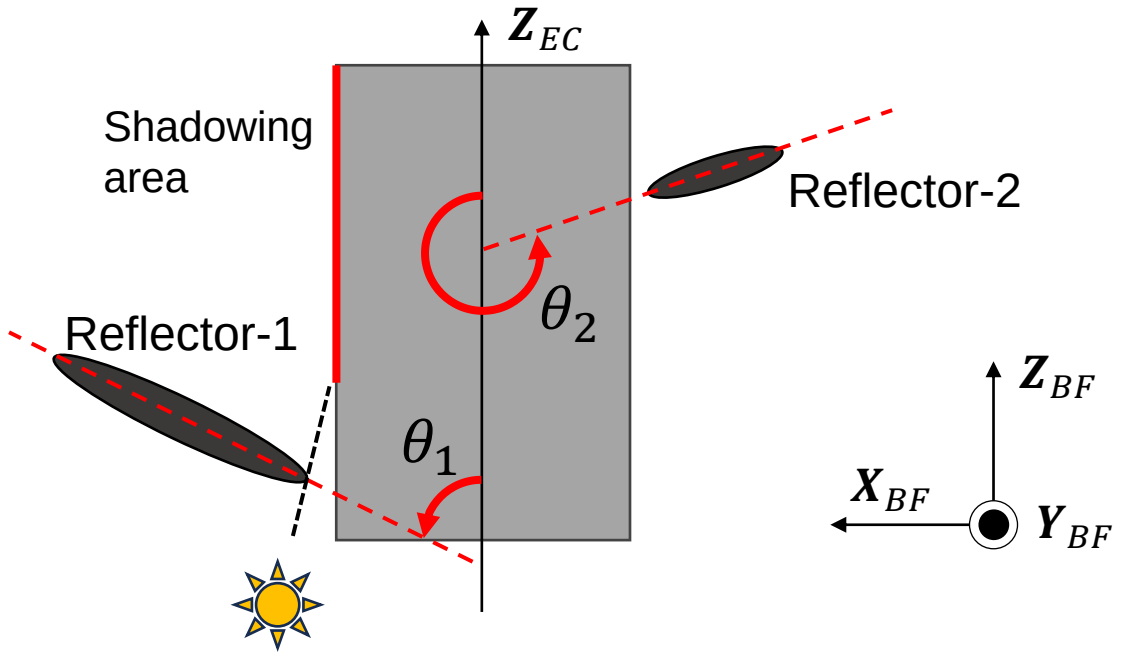

Simplified shadow model for QZS-3

- Example of the shadow area for QZS-3
  - The shadow area projected by or on the reflector-1 reaches 8 m^2 with gap model.
  - The gap between reflector-1 and x surface should be considered.

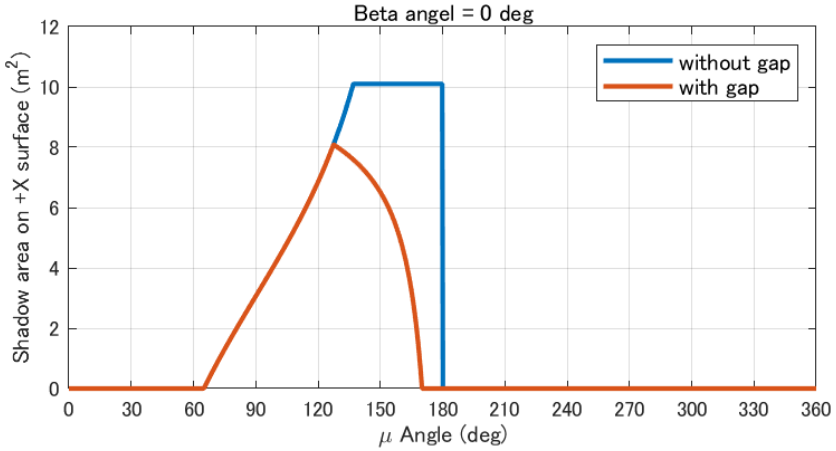

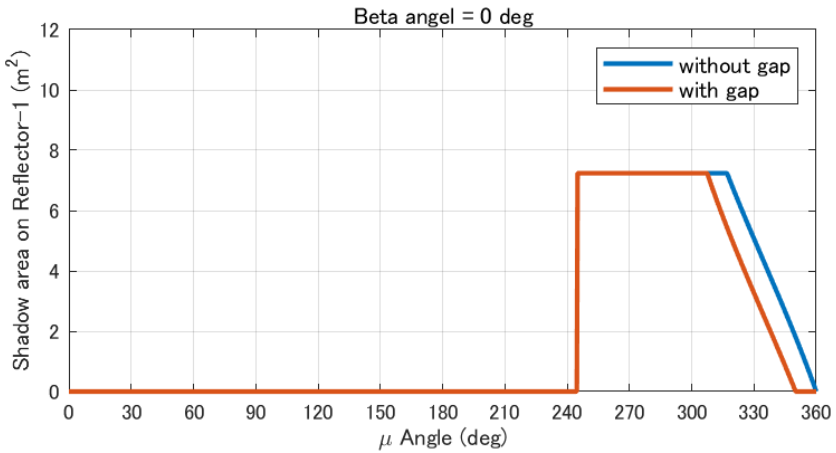

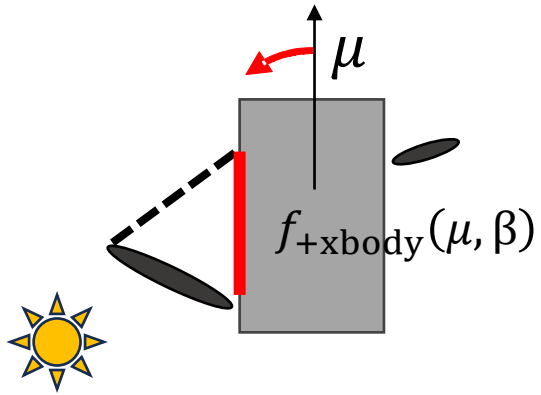

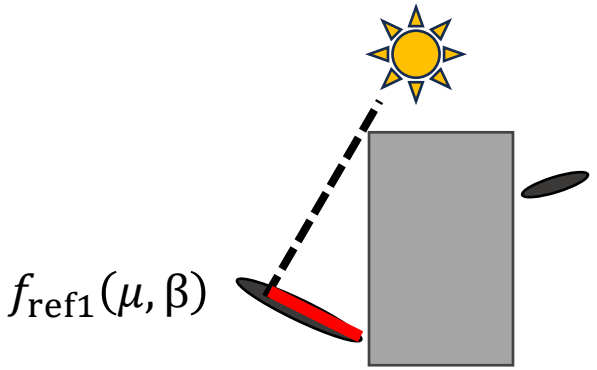

Simplified shadow model for QZS-3

- Beta-angle-dependent effect of the shadowing area
  - To simplify the model, this correction expresses how the area of the shadow on the +x surface cast by the central region of reflector-1 changes depending on the beta angle.

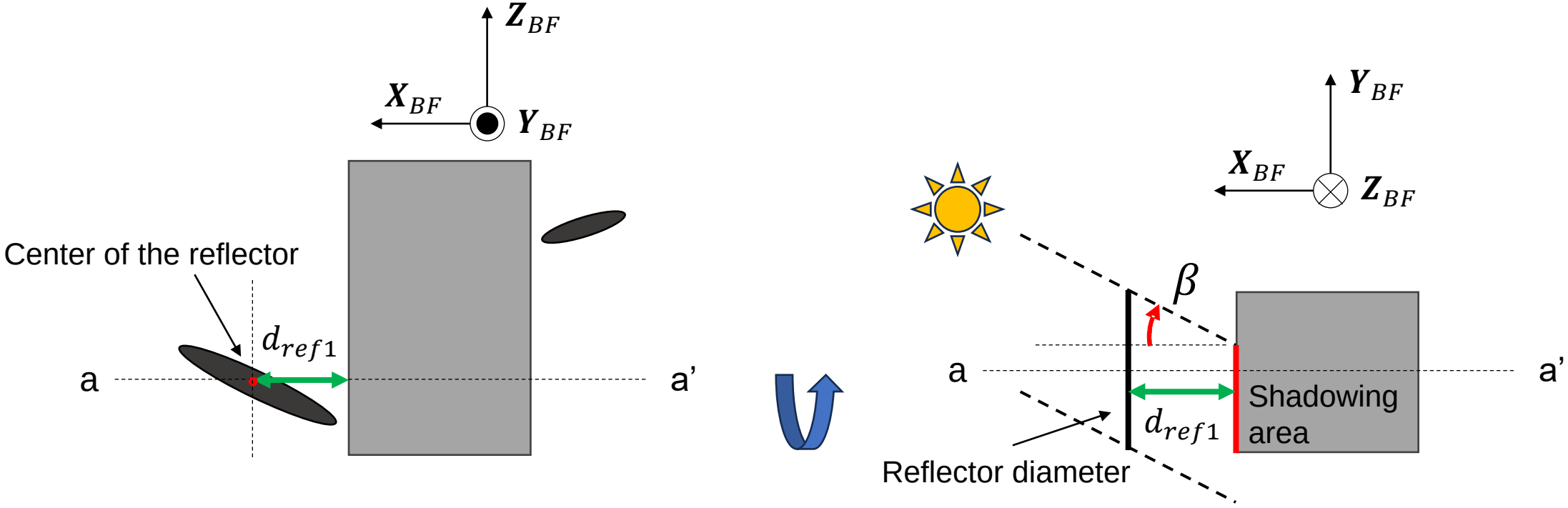

(a) view from +Y axis

(b) view from -Z axis

Model Validation

- Acceleration domain
  - Compared with the acceleration based on the non-disclosed CAD model
  - ECOM parameter estimates

- Precise orbit determination
  - Day boundary discontinuities
  - Daily RMS of linear clock fit residuals
  - SLR residuals

Acceleration compared with CAD-based model in D direction

- Shadow models with the reflector-1 and 2 reduces the inconsistency with the CAD-based model.
- A slight beta angle dependency is still observed after the shadow models applied.

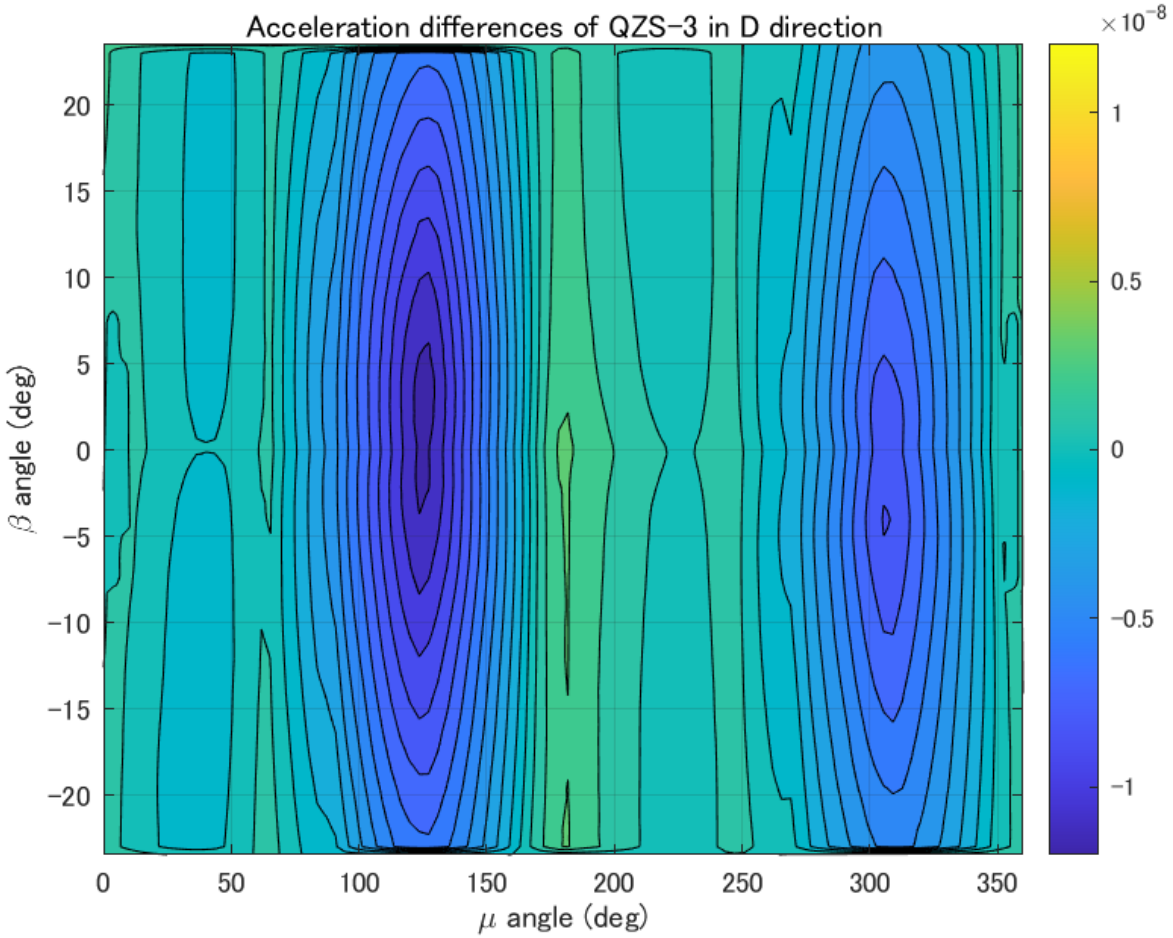

without shadow model

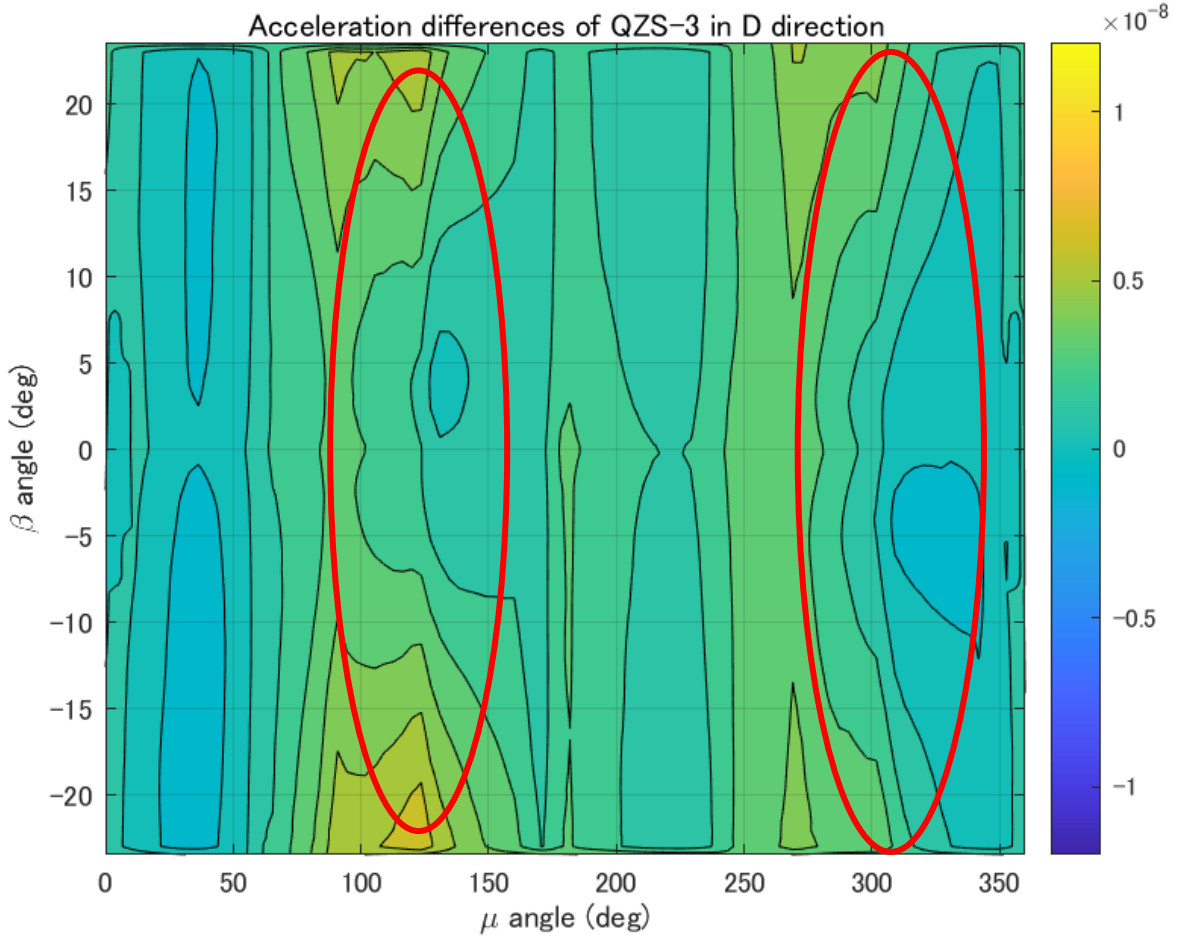

with shadow model (no bata-dependent model)

Acceleration compared with CAD-based model in D direction

- Shadow models with the reflector-1 and 2 reduces the inconsistency with the CAD-based model.
- The beta angle dependency has clearly decreased after the beta-dependent model applied.

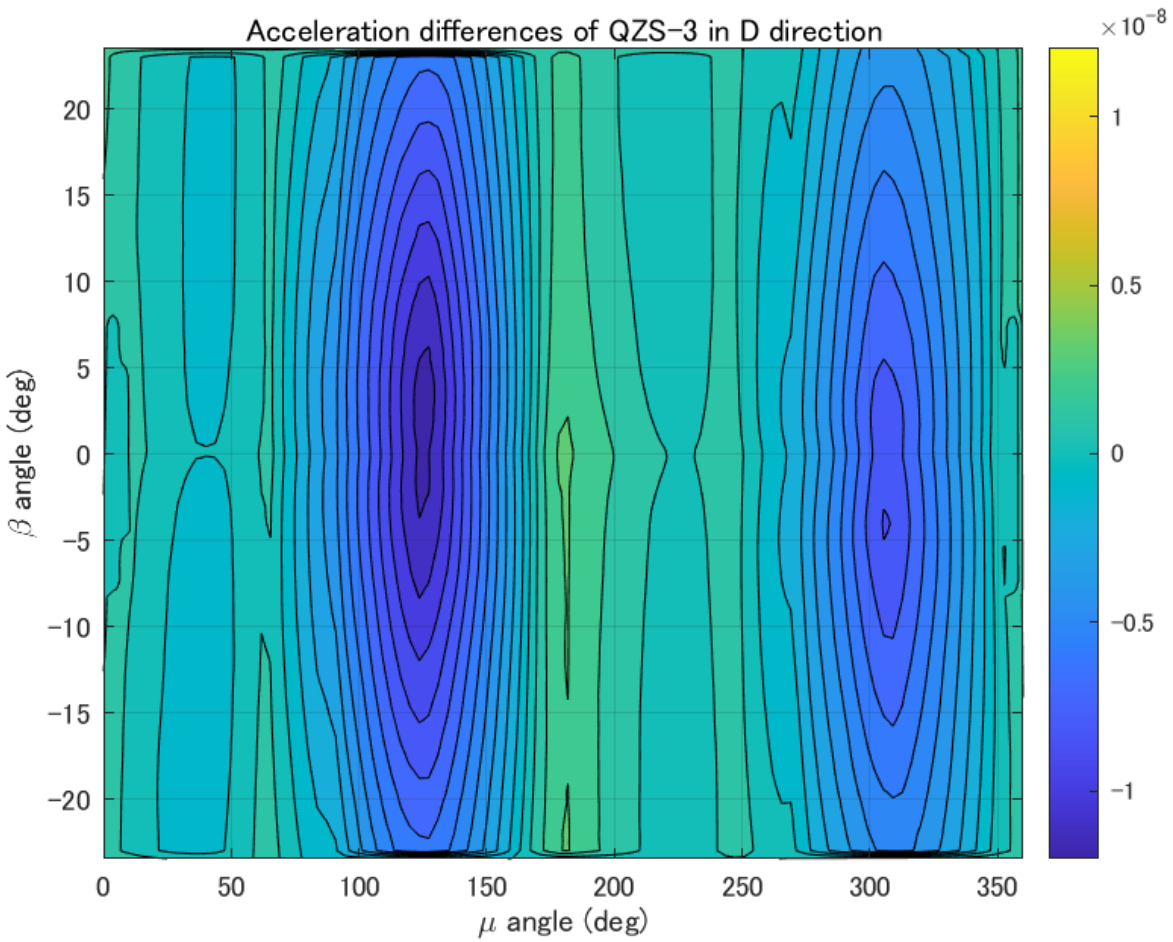

without shadow model

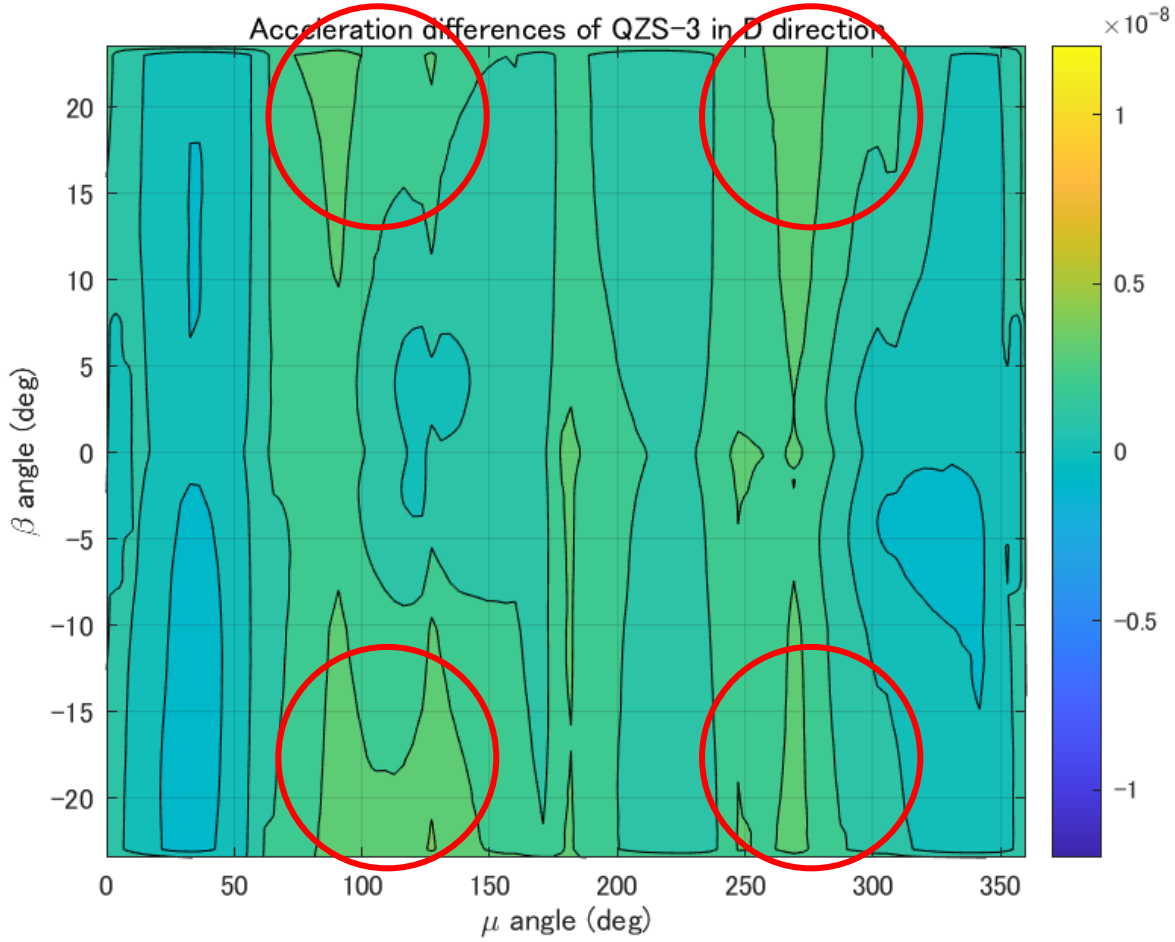

with shadow model (bata-dependent model)

ECOM parameter estimates for QZS-3

- The shadow model for QZS-3 reduced the errors for 2/rev. in D-direction(D2C and D2S).

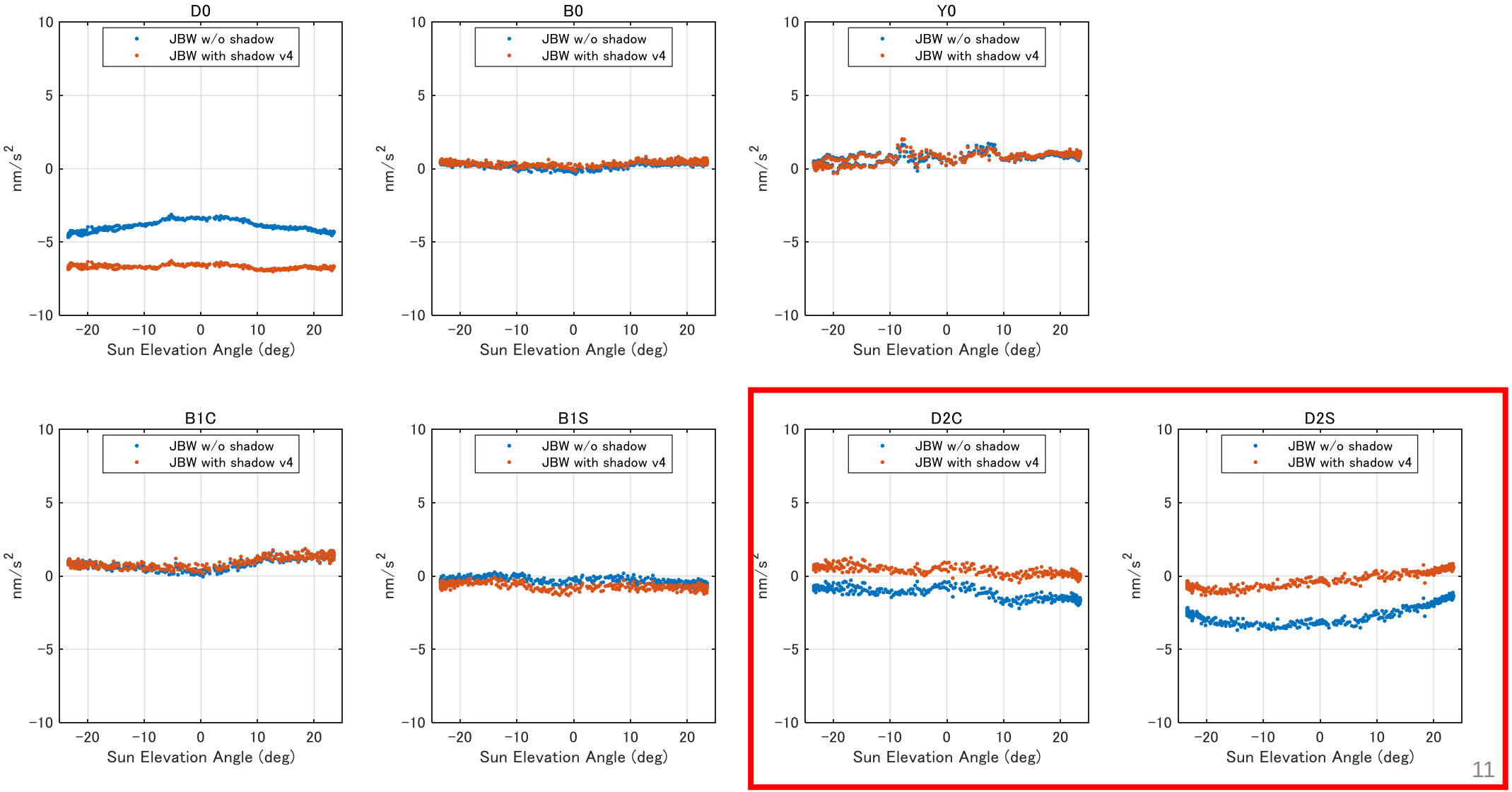

Day boundary discontinuities (DBD)

- The model improves DBD in radial direction by about 20%.
- No beta angle dependency is observed.

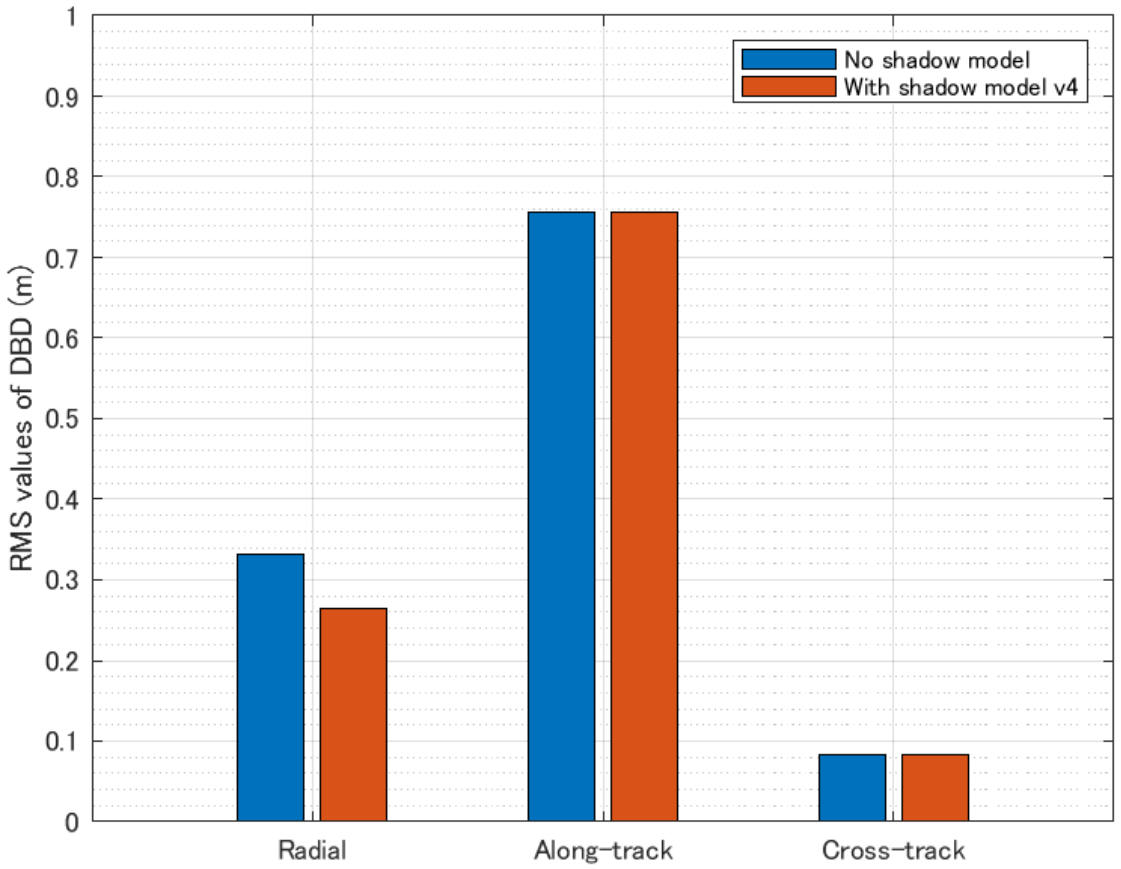

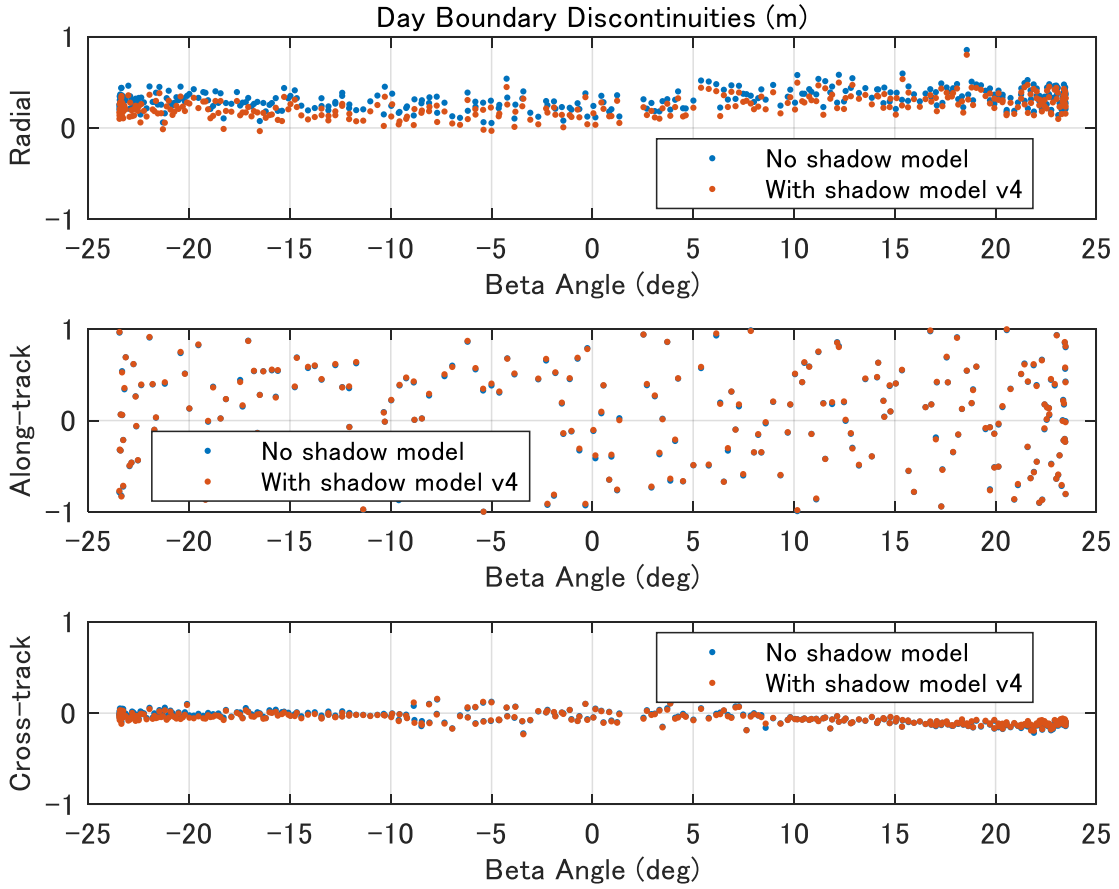

Daily RMS of linear clock fit residuals

- The residuals are computed by fitting the satellite clocks with a linear function during 1-day period.
- The model improves the residuals by about 13%.

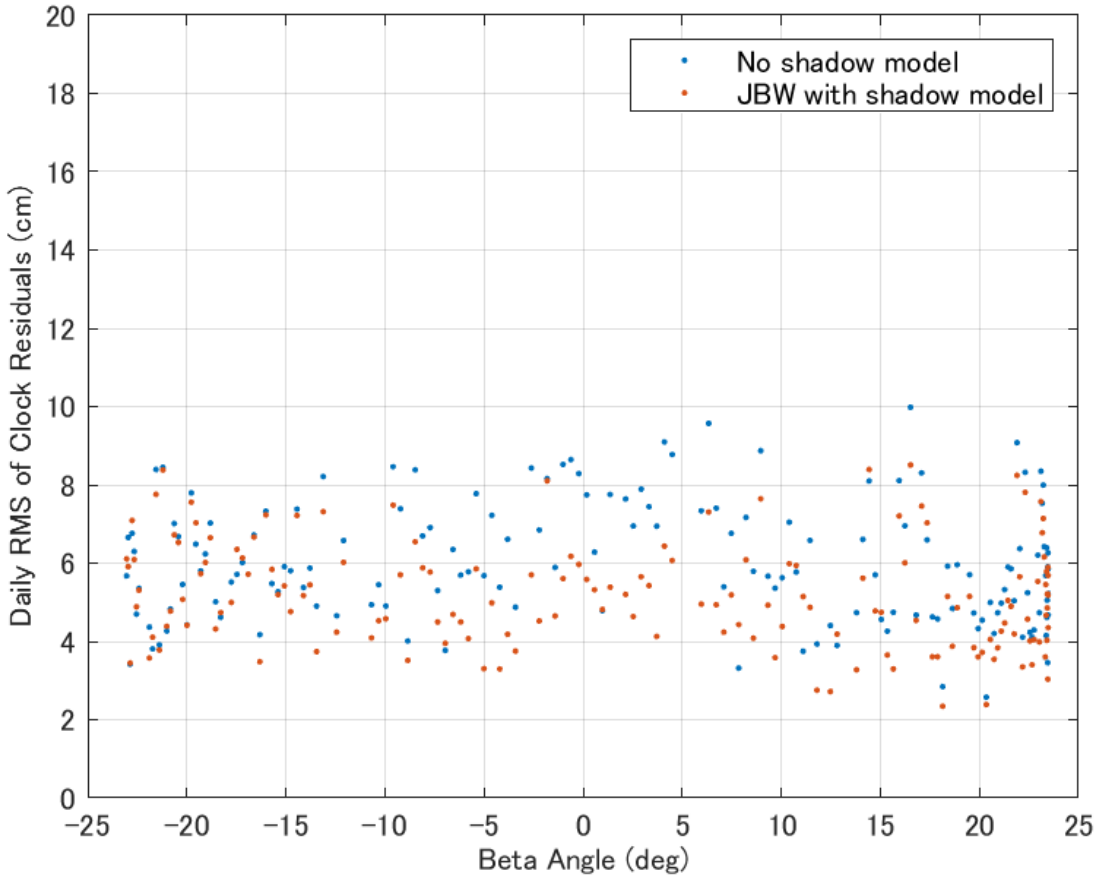

Average value of the daily RMS

- 6.2 cm (no shadow model)
- 5.4 cm (with shadow model)

SLR residuals

- The shadow model improved the STD slightly but increased the offset.
- Some other improvement other than the shadow model is needed!

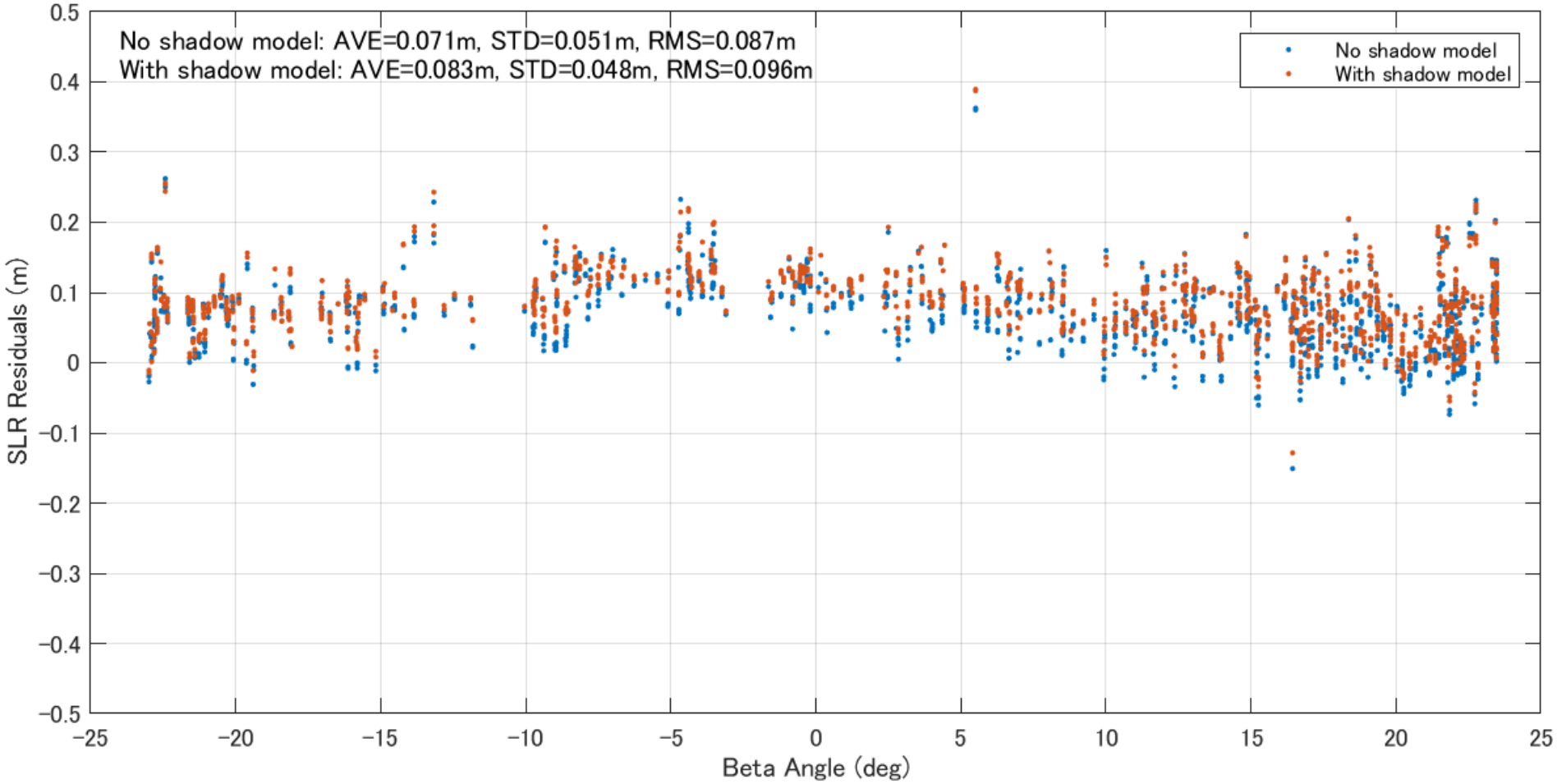

Summary

- Simplified shadow model for large antennas
  - Applicable to satellites in geostationary orbit (e.g., QZS-3 and BDS GEO)
  - Easy to install to conventional box-wing model
  - Using only disclosed data

- Model validations
  - Shadow models for QZS-3 reduces the acceleration errors twice per orbital period in sun direction mainly due to the large reflector.
  - The model improved the day boundary discontinuities (DBD) in radial direction and RMS of linear clock fit residuals by 20 % and 13 %.

Appendix

Simplified shadow model for QZS-3

- Shadow effect in $f_{+xbody}(\mu, \beta)$
  - The area of shadow cast on the +x surface of the body by the reflector-1.

$$f_{+xbody}(\mu) = \begin{cases} \acute{l}_{xw}\left[min(l_{xl}, \acute{l}_{ref1}) - \underbrace{min(l_{xl}, x_{gap1})}_{\text{Gap model}}\right] & (\theta_1 < \mu < \pi) \\ 0 & (otherwise) \end{cases}$$

$$\acute{l}_{xw} = min(l_{xw}/2, l_{ref1}/2 - d_{ref1}tan\beta) + min(l_{xw}/2, l_{ref1}/2 + d_{ref1}tan\beta)$$ * Beta-dependent effect

$$\acute{l}_{ref1} = \frac{(l_{ref1}+l_{gap1})\, sin(\mu - \theta_1)}{sin(\pi - \mu)}$$

$$x_{gap1} = \frac{l_{gap1} sin(\mu - \theta_1)}{sin(\pi - \mu)} \qquad d_{ref1} = \frac{l_{ref1} + l_{gap1}}{2} cos(\pi/2 - \theta_1)$$

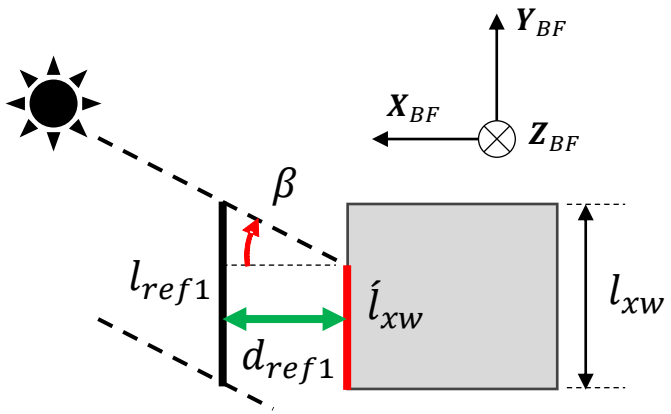

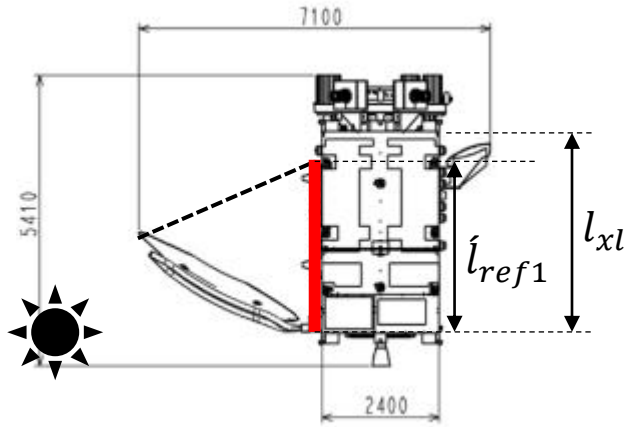

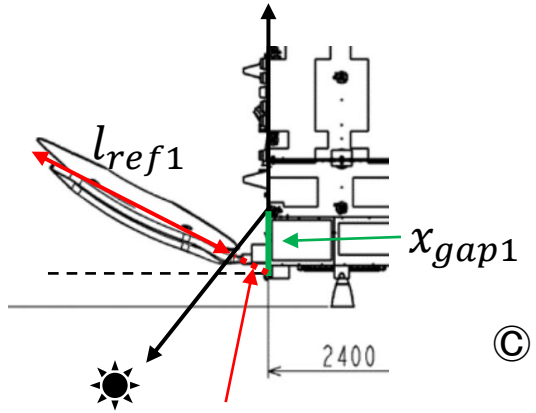

$l_{gap1} \cong 0.75\ (m)$

Simplified shadow model for QZS-3

- Shadow effect in $f_{\mathrm{ref1}}(\mu, \beta)$
  - The area of shadow cast on the surface of reflector-1 by the +x surface of the body.

$$f_{ref1}(\mu) = \begin{cases} \acute{l}_{ref1} min\left(l_{ref1}, \acute{l}_{xl}\right) & (\theta_1 + \pi < \mu < 2\pi) \\ 0 & (otherwise) \end{cases}$$

$$\acute{l}_{xl} = max\left(\frac{l_{xl} sin(2\pi - \mu)}{\sin[\mu - (\theta_1 + \pi)]} - l_{gap1}, 0\right)$$

$$\acute{l}_{ref1} = min\left(l_{ref1}/2\,, l_{xw}/2 - \mathrm{d}_{\mathrm{ref1}} tan\beta\right) + min\left(l_{ref1}/2\,, l_{xw}/2 + \mathrm{d}_{\mathrm{ref1}} tan\beta\right)$$

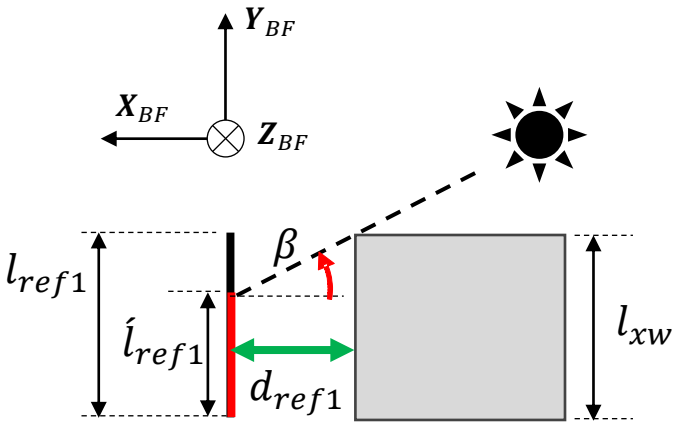

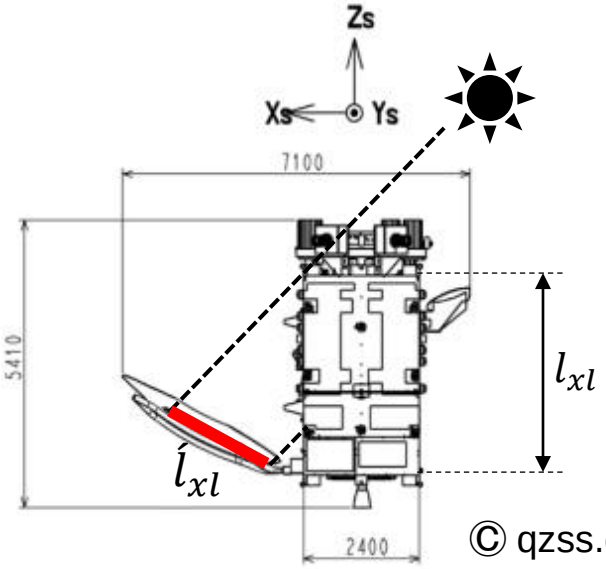

© qzss.go.jp

Simplified shadow model for QZS-3

- Shadow effect in $f_{-xbody}(\mu, \beta)$
  - The area of shadow cast on the -x surface of the body by the reflector-2.
  - l_{gap2} may be made of non-transparent material, the following equation assumes that sunlight does not pass through the area.

$$f_{-xbody}(\mu) = \begin{cases} l_{ref2} min(l_{xl2}, \acute{l}_{ref2}) & (\pi < \mu < \theta_2) \\ 0 & (otherwise) \end{cases}$$

$$\acute{l}_{ref2} = \frac{(l_{ref2} + l_{gap2}) sin(\theta_2 - \mu)}{sin(\mu - \pi)}$$

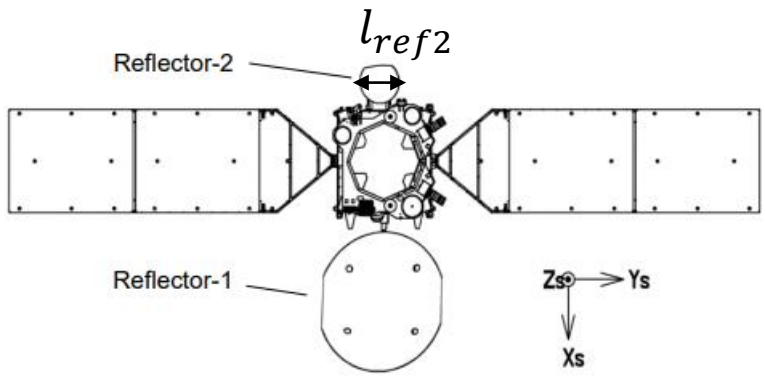

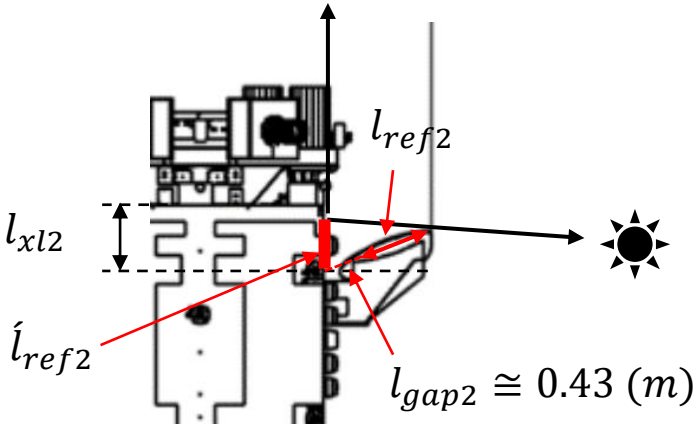

© qzss.go.jp

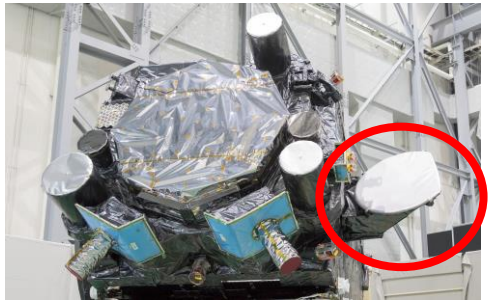

© qzss.go.jp

Simplified shadow model for QZS-3

- Shadow effect in $f_{\mathrm{ref2}}(\mu, \beta)$
  - The shadow area cast by the -x plane on the front and back side of the reflector-2 depends on the length of the shadow's length h

$$\mathrm{h} = \begin{cases} \max\left(\dfrac{\mathrm{l_{xl2}}\sin(\mu)}{\sin[(\theta_2 - \pi) - \mu]} - \mathrm{l_{gap2}}, 0\right) & (0 < \mu < \theta_2 - \pi \text{ for front side}) \\ \max\left(\dfrac{(\mathrm{l_{xl}} - \mathrm{l_{xl2}})\sin(\pi - \mu)}{\sin[\mu - (\theta_2 - \pi)]} - \mathrm{l_{gap2}}, 0\right) & (\theta_2 - \pi \le \mu < \pi \text{ for back side}) \\ 0 & (\text{otherwise}) \end{cases}$$

$$f_{ref2}(\mu) = l_{ref2} min\left(l_{ref2}, h\right)$$

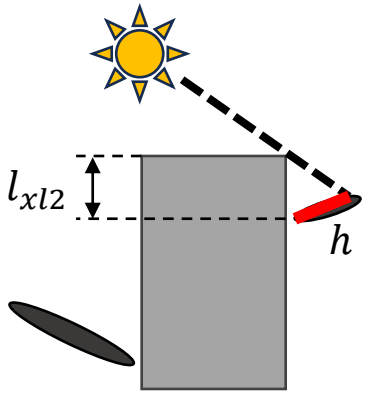

$0 < \mu < \theta_2 - \pi$ for front side

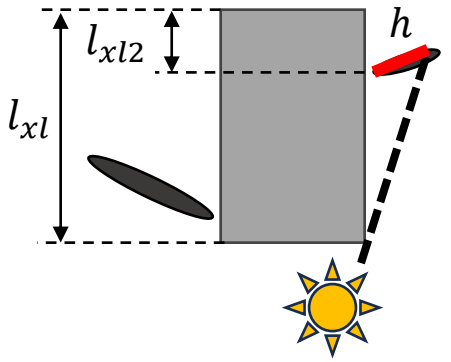

$\theta_2 - \pi \le \mu < \pi$ for back side